

Anhydride-based chemistry on graphene for advanced polymeric materials

1. Details on the general experimental techniques employed

IR spectra were recorded on a Perkin–Elmer System 2000 FTIR spectrometer (Perkin-Elmer Ltd, Beaconsfield, U.K.). The samples were dispersed in KBr and compressed pellets were prepared for analysis in the spectral range between 4000-500 cm^{-1} at a spectral resolution of 4 cm^{-1} .

Raman measurements were undertaken in the Raman Microspectroscopy Laboratory of the Characterization Service in the Institute of Polymer Science & Technology, CSIC. A Renishaw *InVia* Reflex Raman system (Renishaw plc., Wotton-under-Edge, U.K.) was used employing a grating spectrometer with a Peltier-cooled charge-coupled device (CCD) detector, coupled to a confocal microscope. All spectra were processed using Renishaw WiRE 3.3 software. The Raman scattering was excited using an argon ion laser ($\lambda_0 = 514.5 \text{ nm}$) and focused onto the sample with a 50x microscope objective (N.A. = 0.75), with a laser power at the sample of approximately 2 mW.

A computer controlled microscope Intel QX3 was used for contact angle measurements. Samples were placed on a manually controlled tilt table that was back-illuminated with a white light source. With the microscope in a horizontal position, the shape of quiescent water drops of $\sim 3.5 \mu\text{L}$ on the surface was recorded using a 60x objective.

Scanning electron microscopy (SEM) images of cryogenically fractured samples were recorded with a SU8000 Hitachi scanning electron microscope in the Characterization Service of the Institute of Polymer Science & Technology.

Thermogravimetric analysis was undertaken using a TA Instruments Q50 thermobalance, between 50–800 °C at a heating rate of 10 °C min⁻¹ under an inert atmosphere (nitrogen, 60 cm³.min⁻¹). For isothermal measurements, the samples were heated at a scan rate of 10 °C min⁻¹ from room temperature to 650 °C and maintained at that temperature during 8 h, or until constant weight was achieved.

DC-Conductivity measurements were carried out using the four-probe method on films. The hot-pressed films were cut into rectangles (about 0.6 cm wide and 1.2 cm long) and dried under vacuum for 24 h. The measurements were carried out using a four-probe setup equipped with a DC low-current source (LCS-02) and a digital micro-voltmeter (DMV-001) from Scientific Equipment & Services (India).

The crystallization and melting behavior of iPP and iPP-G were investigated by differential scanning calorimetry (DSC) employing a Perkin Elmer DSC7/UNIX/7DX system. The experiments were carried out under nitrogen atmosphere on samples of ~10 mg sealed in aluminum pans. The samples were heated from 40 to 210 °C, maintained at this temperature for 5 min to erase the thermal history of the material, then cooled to 40 °C and heated again to 210 °C. Heating and cooling rates of 10 °C min⁻¹ were used in all cases.

Tensile properties of the composites were measured with an Instron 4204 tensile tester at room temperature and 50 ± 5% relative humidity, using a crosshead speed of 10 mm.min⁻¹ and a load cell of 100 N. Five specimens for each type of composite were tested to ensure reproducibility.

2. Modification of CVD-Graphene

CVD-graphene on Si/SiO₂ was purchased from Graphenea. Succinic acid (SA > 99%) was obtained from Aldrich and used without further treatment.

The modification of graphene with acylium ions was carried out as follows: the CVD-graphene on the Si/SiO₂ wafer (7 mm²) was immersed in a 20 mg.mL⁻¹ solution of succinic

acid in cyclohexanone (CH). Then, 100 mg of Cl_3Al was added to the reactor and the mixture maintained at 60 °C without stirring for 24h. The surface of the wafer was washed with ethanol and abundant water. Maintaining the wafer in quiescent conditions during the reaction was with a view to reduce the possibility of peeling of the graphene from the surface due to shear of the reaction mixture at the surface. Due to the nature of the preparative process to obtain CVD-graphene on Si/SiO₂, after transfer from a metallic (Cu) substrate, the graphene monolayer is only relatively weakly coupled to the Si/SiO₂ surface, due to Van der Waals forces promoted by its very flat surface topology. Therefore detachment of graphene is highly probable when: i) harsh conditions (heat, stirring) are used, or ii) a very high degree of functionalization is achieved. In fact, previous attempts under stronger conditions (including higher temperatures and magnetic stirring) led to the complete detachment of the graphene layer, impeding the analysis of the modified graphene. Using the aforementioned conditions allows the preservation of the integrity of the graphene laminate over the whole surface, confirmed by Raman microscopy recorded from > 20 points, but also limits the degree of functionalization to lower levels.

Reference experiments were also conducted under the same conditions in the absence of Succinic anhydride to check whether defects are introduced into the lattice of graphene by the reaction protocol. The I_D/I_G ratio calculated from Raman spectrum was practically identical to that observed for CVD-graphene, demonstrating that no defects are created in the absence of anhydride groups.

Infrared reflectance microspectroscopy was unsuccessful in detecting the presence of functional groups on the surface of the modified wafer, due to two main issues: firstly, the low concentration per carbon atom on the modified graphene, and secondly, due to the low IR energy available, since the reflectivity of the CVD-G on Si/SiO₂ surface is poor. The use of a brighter IR source is necessary to be able to monitor the surface functionality, and synchrotron IR experiments are planned.

After modification, the surface properties changed significantly as the CVD-G became more hydrophilic. The water contact angle diminished after the chemical functionalization as shown in Figure S1. The extent of the reduction in the contact angle differs from one zone to other on the piece, due to differences in the degree of functionalization over the surface, probably a consequence of the quiescent conditions. Notwithstanding, it is clear that the modification lead to a significantly more hydrophilic surface.

The effect of the Si/SiO₂ substrate on the WCA is discarded because different values have been measured for Si/SiO₂ (28 - 36 °) and, as mentioned earlier, the graphene laminate is not damaged during the modification.

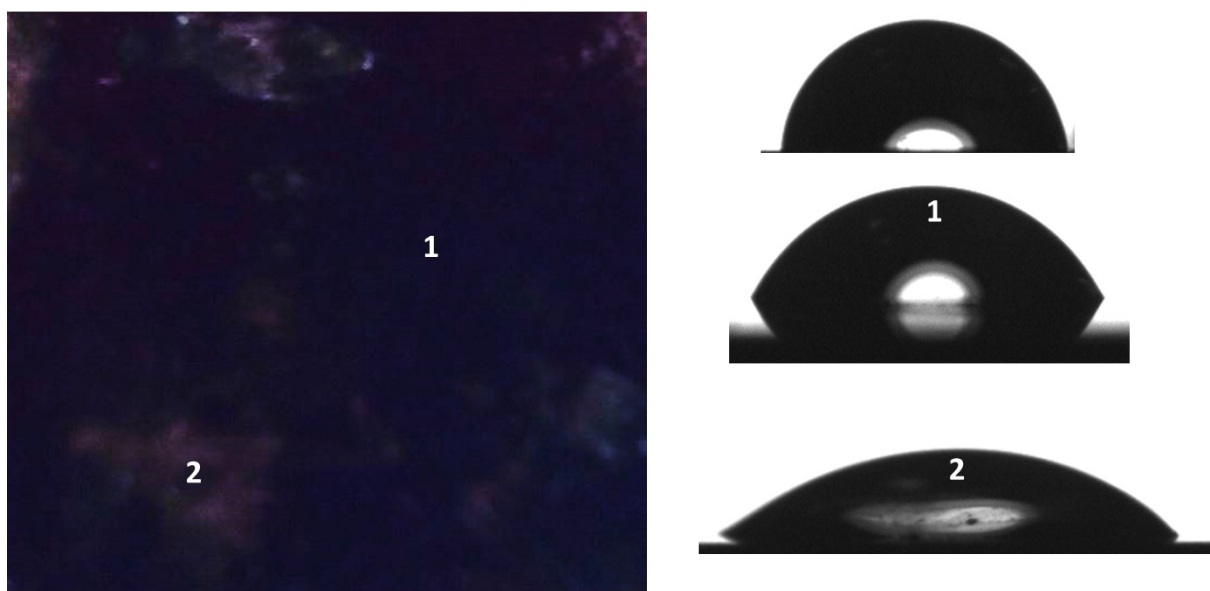


Figure S1. (A) Water contact angle of CVD-G before (top) and after coupling of acylium (middle and bottom) collected in the regions marked in (B).

3- Modification of bulk graphene with maleic-anhydride-grafted polymers

3.1 Polypropylene

Graphene nanoplateles (GNP), 6-8 nm were purchased from io-li-tec Nanomaterials. Polypropylene-graft-maleic anhydride (PP-MA, Mw ~ 9100; maleic anhydride content 8-10 wt. %) was obtained from Aldrich. The solvents were stored with NaSO₄ to avoid water

uptake. Anhydrous NMP and xylene were used as received and cyclohexanone (CH) was previously distilled.

The bulk modification of graphene with PP-MA was accomplished in warm NMP. Briefly, 50 mg of GNP were dispersed in anhydrous NMP; then 2 g of PP-MA (0.18 g of MA) were dissolved in xylene at 100 °C and added to the graphene dispersion. Subsequently, 300 mg of Cl_3Al were added and the mixture was maintained overnight at 110 °C under stirring. The mixture was left to cool and the precipitate that formed was filtrated and washed with warm xylene, to remove any non-reacted polymer, and methanol.

The Raman spectra of graphene, neat PP-MA and the graphene-modified product (G-PP) are shown in Figure S2.

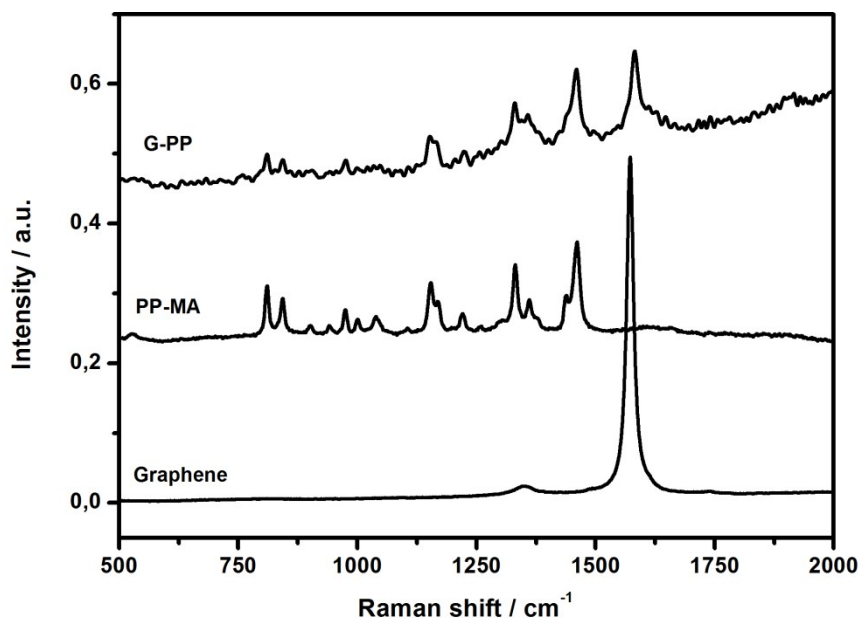


Figure S2. Raman spectra of graphene, PP-MA and the coupling product of them. $\lambda = 514$ nm.

Full details on the spectroscopic characterization of the modified graphene are also given in Table S1 from which the success of the modification is confirmed.

Table S1. Summary of the FTIR and Raman bands of iPP with corresponding assignments according to the literature¹.

FTIR frequency / cm^{-1}	Raman frequency / cm^{-1}	Assignment
1460	1457	δCH_3 asym + δCH_2
	1436	δCH_3 asym
1377		δCH_3 sym + CH_2 wag
1358	1361	CH_3 sym bending + σCH
1305		ωCH_2 + tCH_2
1256		δCH + tCH_2 + rCH_3
	1220	tCH_2 + δCH + $\nu\text{C-C}$
1169	1170	$\nu\text{C-C}$ + rCH_3 + δCH
	1153	$\nu\text{C-C}$ + $\nu\text{C-CH}_3$ + δCH + rCH_3
1102		$\nu\text{C-C}$ + rCH_3 + ωCH_2 + tCH + δCH
	1041	$\nu\text{C-CH}_3$ + $\nu\text{C-C}$ + δCH
998	1000	rCH_3 + ωCH_2 + δCH
973	976	rCH_3 + $\nu\text{C-C}$ chain
	941	rCH_2 + $\nu\text{C-C}$ chain
898	903	νCH_3 + rCH_2 + δCH
842	841	rCH_2 + $\nu\text{C-CH}_3$
808	812	νCH_2 + $\nu\text{C-C}$ + $\nu\text{C-CH}$

3.2 Poly(vinyl chloride)

In the case of poly(vinyl chloride)(PVC) the commercial sample employed did not have anhydride moieties. Therefore the commercial PVC was functionalized using the method displayed in Scheme S1.

The PVC sample used was an additive-free commercial-grade PVC from Atochem, Spain ($M_n \sim 44.000 \text{ g}\cdot\text{mol}^{-1}$), obtained by bulk polymerization at 70°C ; the polymerisation process being stopped at a conversion of 62%.

Substitution Reaction of PVC with NaN_3 (PVC- N_3)

2.0 g (32.0 mmol, based on monomeric unit) of PVC was dissolved in 100 mL of CH. Then 2.35 g (36.2 mmol) of NaN_3 in 150 mL of CH was added to the polymer solution. The mixture was stirred and heated at 60°C under inert atmosphere. At appropriate reaction times,

concentrations of MA and polymer were maintained constant. We have developed a method that combines the two modifications of the PVC. This method includes grafting MA onto PVC chains (PVC-MA) in solution under the controlled thermal decomposition of the azide group. The results confirm that the efficiency of the reaction is quite similar to that obtained by means of the two-step synthesis, which improves the overall yield of the reaction

The overall composition of MA-functionalized samples was determined by FTIR and ^1H NMR. Anhydride content was determined by reference to a calibration curve prepared with a PVC-MA adduct. The composition of the grafted MA group was determined from the ratio of absorbance between bands at 1780 cm^{-1} and 1428 cm^{-1} . Films of azide-modified PVC and MAH-functionalized samples were prepared by casting from dilute THF solution ($40\text{ mg}\cdot\text{mL}^{-1}$). After slow evaporation at room temperature the films were dried in vacuum.

Grafting Graphene to Modified PVC-MA

0.4 g of PVC bearing $\sim 4\text{ wt. \%}$ of MA groups was dissolved in 20 mL of CH. Then, 50 mg of AlCl_3 and 20 mg of GNP dispersed in 30 mL of CH were added to the polymer solution. The mixture was stirred and heated at 60°C under a stream of oxygen-free nitrogen during 48 h. The solid product was collected by filtration and thoroughly washed with methanol, water, and HCl and subsequently dried to constant weight at 40°C under reduced pressure.

The success of the reaction was confirmed by FTIR, as in the case of polypropylene, although the changes observed here were less marked (Figure S3). A clear decrease in the intensity of the asymmetric (1780 cm^{-1}) and symmetric (1735 cm^{-1}) C=O stretching vibrations of the anhydride group, and the C=O vibration of esters (1680 cm^{-1}) is observed.

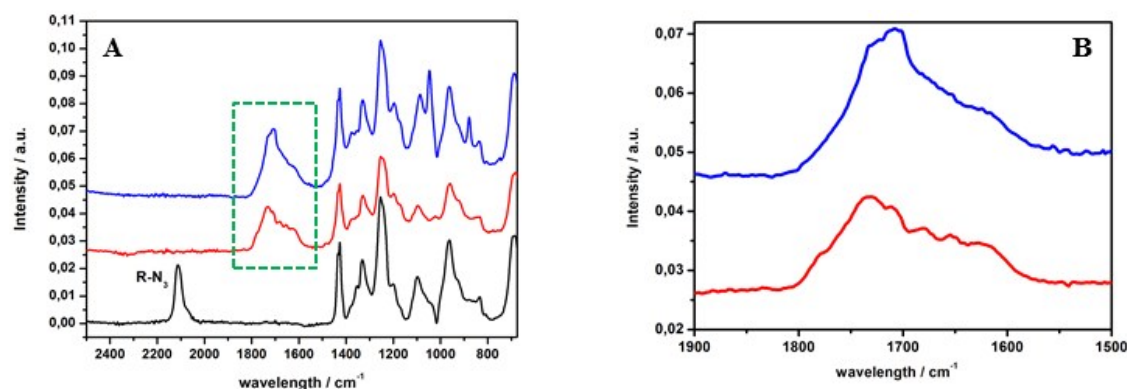


Figure S3. (A) FTIR spectra monitoring the modification of PVC by the three steps described above: azide- PVC (black trace), succinic anhydride-PVC (red) and G-PVC (blue). An enlarged view of the carboxylic region for the latter two is shown in (B).

4. Preparation of nanocomposite of iPP with G-PP.

As the objective here was to employ the covalent product (G-PP) as a filler in neat iPP. A covalent material, G-PP with a much higher content of graphene was prepared following the procedure described in section 3.1 but with a much higher Graphene/PP-MA ratio in the feed (0.8 g of graphene and 0.4 g of PP-MA). The final graphene content, determined from the residual mass in TGA, was 77 wt. % (Figure S4), suggesting that the filler contained 23 wt. % of polypropylene chains that could contribute directly to the improvement of the interphase with the iPP matrix.

The preparation of the G-PP/iPP nanocomposite, with 5 wt. % of filler (3.7 wt. % of graphene), was accomplished by two consecutive mixing steps. Firstly, 300 mg G-PP was mixed for 1 hour with the appropriate amount of polypropylene in warm xylene (110 °C) under vigorous stirring. Subsequently, the mixture was precipitated in methanol, filtered and washed with methanol and dried under vacuum. Secondly, both components were further mixed by melt-blending processing. The melt-blending was performed in a Haake Minilab extruder operating at 210 °C, with a rotor speed of 150 rpm, using a mixing time of 5 minutes. The extruded material was used to fabricate thin films (~ 500 μm thick) by hot-compression, under successive pressure steps of 0, 25 and 60 bars, for periods of 6 minutes for the first step

and 5 minutes for the rest. A brass frame was employed to control the dimensions, and two flat brass plates were used as top and bottom surfaces to guarantee uniform thickness of the films.

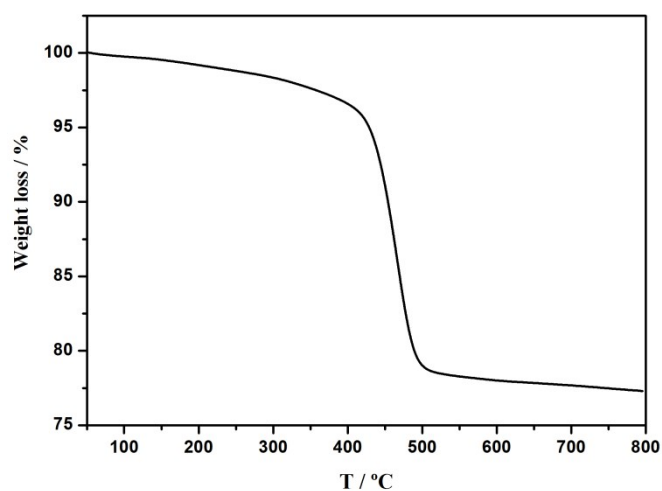


Figure S4. TGA curve of the G-PP product prepared to be used as filler of pure iPP. The curve was collected under N₂ atmosphere at a scan rate of 10 °C.min⁻¹

The nanocomposite presents improved properties with respect to iPP. Figure S5 shows the TGA curves for iPP and iPP/G-PP, where a remarkable delay in the onset of degradation and an increase of the temperature of degradation rate are evident.

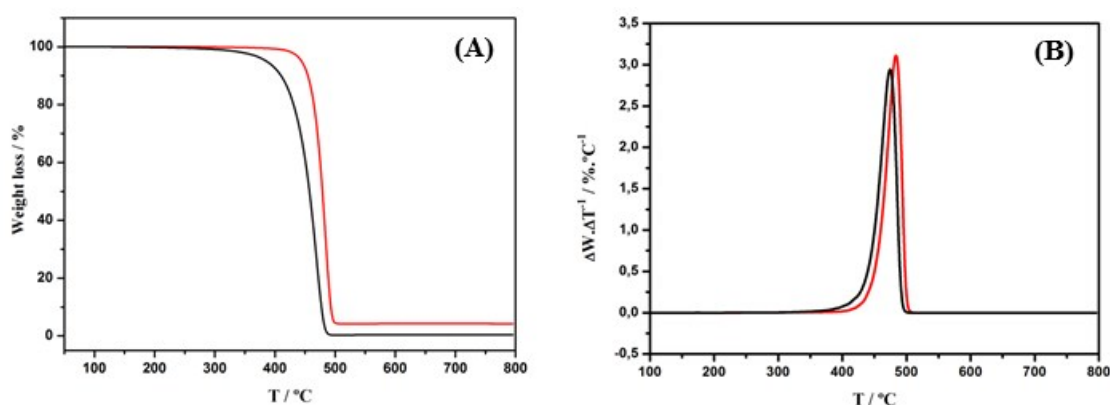


Figure S5. TGA (A) and dTGA (B) curves for pure iPP (black trace) and its nanocomposite with 3.7 wt. % of graphene (5 wt. % of G-PP, red) under N₂ atmosphere. Scan rate = 10 °C.min⁻¹

Physical changes in the iPP and the nanocomposite with 5 wt. % of G-PP are shown in Figure S6. The first cooling scan shows a clear nucleating effect due to the presence of modified graphene (Figure S6b), with an increase in crystallization temperature (T_c) from 113 °C for iPP to 124 °C for the nanocomposite. In addition, an increase in the melting temperature (T_m) and a slight change in the degree of crystallinity are also observed (Figure S6a).

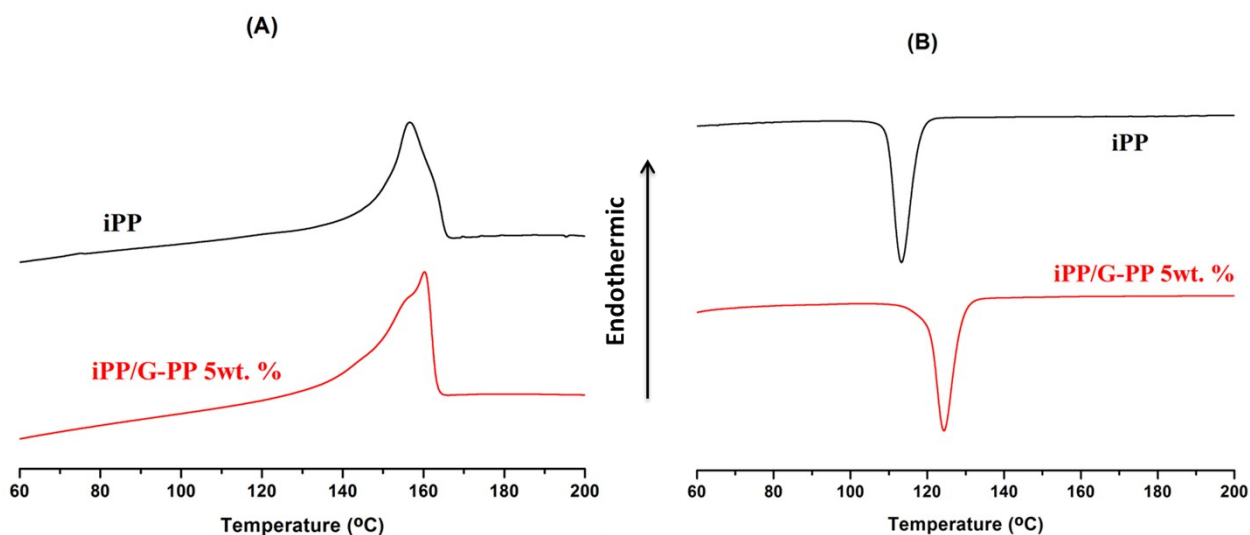


Figure S6. Thermal behavior of iPP and G-PP/iPP: DSC heating (A) and cooling (B) scans at $10\text{ °C}\cdot\text{min}^{-1}$.

Finally the presence of graphene causes clear changes in the mechanical properties, such as the Young's modulus that increases significantly from $660 \pm 30\text{ MPa}$ for iPP to 1354 ± 125 for the nanocomposite (Table S2)

Table S2. Variation of the mechanical properties of iPP and G-PP/iPP nanocomposites

	<i>Young Modulus (MPa)</i>	<i>Strain at break (%)</i>	<i>Tensile Strength at break (MPa)</i>
iPP	660 ± 30	11.5 ± 1.5	24 ± 7
iPP/G-PP 5 wt. %	1354 ± 125	2.4 ± 0.3	14 ± 2

Finally, the electrical conductivity was calculated as the inverse of the resistivity (ρ), expressed by the following equation:

$$\rho = 4.5234 t \left(\frac{V}{I}\right) f_1 f_2 \quad (2)$$

where t is the thickness of the sample (cm), I is the intensity (A), V is the measured potential (V), and f_1 is the finite thickness correction for thick samples on an insulating bottom boundary and f_2 is the finite width correction.

References

-
- [1] M. Arruebarrena de Báez, P. J. Hendra and M. Judkins, *Spectrochimica Acta Part A: Molecular and Biomolecular Spectroscopy*, 1995, **51**, 2117-2124.
- [2] G. Martínez, *J. Polym. Sci. A: Polym. Chem.* 2006, **44**, 2476